NEUVIEME COLLOQUE SUR LE TRAITEMENT DU
SIGNAL ET SES APPLICATIONS

NICE du 16 au 20 MAI 1983

DIGITAL MULTIFREQUENCY RECEIVERS USING NONLINEAR SPECTRAL ESTIMATION

Bulent Sankur* and Willem Steenaart

University of Ottawa
Department of Electrical Engineering
Ottawa, Ontario K1N 6N5 Canada

RESUME

Le récepteur à multiples fréquences est une composante importante pour l'interface entre des réseaux analogues et numériques. De nouvelles solutions au problème du récepteur à multiples fréquences ont été etudiées. Les nouvelles solutions sont basées sur l'estimation paramétrique d'un spectre autoregressive. Les spectres sont estimés à partir d'échantillons de longueurs finies. Les diverses fréquences sont obtenues en détectant la position des maximums et le contenu énergétique des valeurs pointes.

Cette étude est basée sur les résultats de simulations pour diverses combinaisons de fréquences et de bruit. Les performances des algorithmes d'estimation des spectres ont été classées en fonction de leurs probabilités d'erreurs et de leurs efficacités en fonction de la taille de l'échantillonnage. L'estimation de spectres autorégressifs par la methode d'auto correlation s'avère être une alternative intéressante au problème de la détection de fréquence par rapport aux solutions existantes. De nouveaux développements dans l'application de cette technique sont à suivre.

SUMMARY

An important component in the interface between analog and digital networks is the multifrequency receiver. New solutions to the multifrequency receiver problem have been investigated. These solutions are based on parametric spectrum estimation techniques of the autoregressive variety. The spectra are estimated based on a finite sample size and the tones are detected by searching the location and energy content of the peaks.

This study has been based on simulation results for various signalling frequency combinations and noise conditions. The performance of the spectral estimation algorithms have been ranked with respect to their probability of error performance and sample efficiencies. The autocorrelation method of estimating the autoregressive spectrum has been found to be a viable alternative to existing solutions for the tone detection problem. Further progress in the realization of this technique is to follow.

1. INTRODUCTION

Direction and control of automatic switching machines in telephony are carried out through tone signalling. Tones can be used for multifrequency signalling in a data set, Touch-Tone^{R} signalling, milliwatt tone testing and in a variety of information signalling functions such as address, busy, idle, seizure, disconnect signals and audible ring, dial tones, receiver off-hook signal, etc.

Conventional analog multifrequency (MF) receivers are handicapped for various reasons, i.e., they are subject to thermal aging, fine initial adjustments are required, they are inherently large and heavy and the implementation requires a number of LC filters and nonlinear devices. There is therefore considerable interest in developing alternate and efficient digital multifrequency receivers.

The existing digital dual tone multifrequency receivers can be expressed under the following headings: i) Bank of bandpass filters [1], ii) Spectral moment estimation [2], iii) Zero crossing counter [3], iv) Discrete Fourier transform based receiver [4], v) Quadrature detection. In this research we have investigated the effectiveness of various nonlinear spectral estimation techniques for the dual tone mul-

Support from the Natural Sciences and Engineering Research Council under Grant A8572 and Strategic Grant G0665 is gratefully acknowledged.

*Currently on leave of absence from Bogaziçi University, Istanbul, Turkey.

frequency receiver.

2. NOISE BACKGROUND AND DETECTION LOGIC

The most common multifrequency receiver is the dual tone multifrequency (DTMF) receiver where two tone signals at two different frequencies carry the information. The frequency matrix for the Touch-Tone^R DTMF system is shown in Table I.

Table I: Frequency Matrix for the Touch-Tone^R Receiver

Lower Group \ Upper Group	1209	1336	1477	1633
697	1	2	3	5
770	4	5	6	S
852	7	8	9	S
941	*	0	#	S

Noise Background

The tones are imbedded in bandlimited (0-3 KHz) Gaussian noise and contaminated by sporadic outbursts of impulsive noise. The impulsive noise is represented as an additive combination of Gaussian noise and a low density shot process [5]:

$$n(t) = \sum_{k=1}^{K(t)} u_i \, h(t-t_i) + w(t)$$

where $w(t)$ is the Gaussian noise, $\{u_i\}$ are independent identically distributed random variables with common power-Rayleigh distribution:

$$f(u) = \frac{\alpha}{2\sigma^{\alpha}} |u|^{\alpha-1} \exp\{-|u|^{\alpha}\} \qquad \begin{matrix} 0 < \alpha \le 2 \\ -\infty < u < \infty \end{matrix}$$

and $K(t)$ is a Poisson counting process. Finally, $\{h(t)\}$ denotes the shot noise waveform, i.e., typically, $h(t) = \exp(-\alpha t)$, $t \ge 0$. The impulsive noise itself could be originating from arcing during switching, accidental hits during repair and maintenance work and various other sources.

The detection of the tones could also be perturbed by the presence of other signals, i.e., voice digits. This type of error is called digit simulation.

Detection Logic

The tone detection algorithm is based on the estimation of the power spectral density and on testing for the location and energy of the spectral peaks. The detection (or rejection) logic consists of the following stepts: i) The signal magnitude is in the specified range, ii) The difference in the energy level of the tones (twist factor) is in the specified range, iii) The spectrum in the remaining six bands is at least 6 dB below the second largest output from frequency analysis, iv) The estimated tone frequency as determined from the location of the spectral peak is within 3.5% of the actual tone frequancy. These requirements are summarized in Table II.

Table II: Requirements for DTMF Receiver

Allowable frequency deviation	3.5%
Allowable signal level	-3 to -24 dBm
Allowable twist	< 15 dB
Response time	25 to 40 ms
Tone to background separation	> 6 dB
(Gaussian noise, (15 dB, SNR)	$P_e < 1.0 \times 10^{-4}$
Impulsive noise, (15 dB SNR)	$P_e < 1.4 \times 10^{-3}$
Digit simulation(room noise + speech)	$P_e < 3. \times 10^{-4}$

3. ESTIMATION ALGORITHMS AND ACCURACY

In the parameter estimation approach to tone detection one would like to implement the maximum (ML) estimator. The ML parameter estimate for a single tone consists simply of calculating the discrete Fourier transform of a sequence and identifying the peak location and its amplitude. In the presence of several tones, however, the ML parameter estimation is considerably more difficult and involves a tedious nonlinear search. In the quest for suboptimal but viable approaches to tone parameter estimation we conjecture that the parametric power spectrum estimation methods will be an attractive alternative.

Tone Parameter Estimation Accuracy

Under certain regularity conditions, useful bounds on the accuracy of the parameter estimates can be found [6]. Consider the multitone signal in additive noise:

$$r(t) = \sum_{i=1}^{M} A_i \cos(2\pi f_i t + \theta_i) + w(t) \qquad (1)$$

where $w(t)$ is a sample function of a white Gaussian process. Let us denote the parameter vector by $\underline{a}$, i.e., $\underline{a} = [A_1 f_1 \theta_1 A_2 f_2 \theta_2 \ldots]$. The Cramer-Rao bound for the j-th parameter is given by

$$\mathrm{var}\{a_j - \hat{a}_j\} \ge \Sigma^{jj} \qquad (2)$$

where Σ^{jj} is the jj-th element of the inverse of the Fisher information matrix, i.e.,

$$\Sigma_{ik} = -E\{ \frac{\partial^2}{\partial a_i \partial a_k} \log f \, (\underline{r}/\underline{s})\} \qquad (3)$$

with the probability density function

$$f(\underline{r}/\underline{s}) = \frac{1}{(2\pi)^{N/2} |\underline{R}|^{1/2}} \exp\{ -\frac{1}{2} (\underline{r}-\underline{s})^T \underline{R}^{-1} (\underline{r}-\underline{s})\}$$

$\underline{r}$, $\underline{s}$ being, respectively, the sampled vector of the received signal and the pure tones. The Cramer-Rao bounds for the two tone problem are shown in Figures 1 and 2.

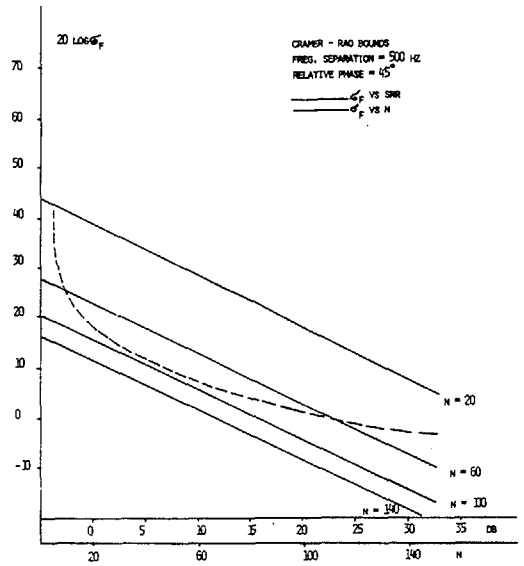

Fig. 1: Cramer-Rao bounds on the frequency estimation accuracy versus the number of data samples used (dashed) and the signal to noise ratio (solid).

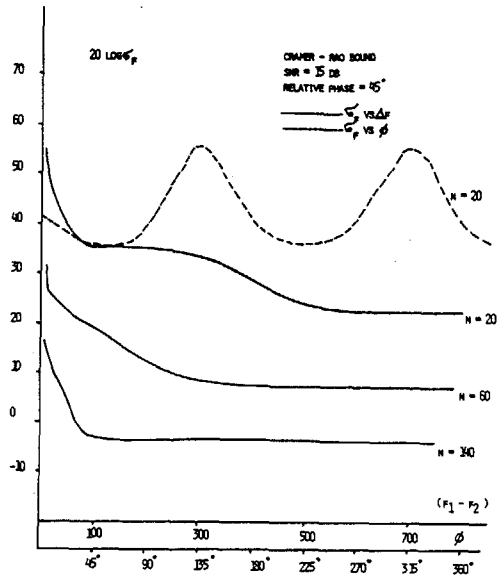

Fig. 2: Cramer-Rao bounds on the frequency estimation accuracy versus frequency separation Δf(solid) and relative phase angle (dashed).

In Fig. 1 the estimation accuracy of the tone frequency, $\sigma_f^2 = E\{(f_i - \hat{f}_i)^2\}$ is plotted versus the number of samples used. For example at a signal to noise ratio (SNR) of 15 dB, the tone frequency can be estimated with a standard deviation of 32 Hz if only 10 samples are used. Otherwise the accuracy improves rapidly with the increased number of samples. Also the variance of the estimate decreases linearly with SNR. In Fig. 2 the estimation accuracy is plotted versus the tone separation. Recall that in typical DTMF's the tone frequency separation is of theorder of 200 Hz or beyond; thus if 60 or more samples are being used (15 dB SNR) the Cramer-Rao bounds behave like that of a single tone. One can note also the non-negligible phase dependence of the bounds.

Estimation Algorithms

Consider the signal $\{s_n\}$ plus noise $\{v_n\}$ sequence

$$x_n = s_n + v_n \,. \tag{4}$$

Linear process models to represent (4)

$$x_n = \sum a_m x_{n-m} + \sum b_m w_{n-m} \tag{5}$$

yield power spectral estimates of the form

$$s(f) = \sigma^2 \left| \frac{b_m z^{-m}|^2}{|1 - a_m z^{-m}|^2} \right|_{z=e^{j2\pi fT}} \tag{6}$$

where the $\{a_m, b_m\}$ coefficients themselves can be determined through various algorithms. Autoregressive (AR) models and various AR parameter estimation techniques have been most popular [7]. In the AR case, the parameter estimation algorithm is particularly simple, as it results in a set of linear equations:

$$\begin{bmatrix} r_0 & r_{-1} & \cdots & r_{-p} \\ r_1 & r_0 & \cdots & \\ \vdots & & & \\ r_p & \cdots & & r_0 \end{bmatrix} \begin{bmatrix} 1 \\ a_1 \\ \vdots \\ a_p \end{bmatrix} = \begin{bmatrix} \sigma^2 \\ 0 \\ \vdots \\ 0 \end{bmatrix} \tag{7}$$

where the elements of the covariance matrix are estimated as

$$r_k = \frac{1}{N} \sum_{n=0}^{N-1} x_{n+k} x_n^* \tag{8}$$

This is referred as the autocorrelation method which causes inherently a windowing of the data as is obvious from (8). This windowing can be avoided by letting the prediction filter run over only the data set, as in the Burg algorithm [7]. While the Burg algorithm uses a constrained minimization to compute the predictor coefficients and guarantees a minimum phase solution, an unconstrained minimization approach results in a more statistically stable estimate. The latter approach is referred to as the least squares (LS) AR parameter estimation.

An improvement on the least-squares method of AR parameter estimation is provided by the Kumaresan-Prony case [8]. It can be shown that the minimum norm solution for the predictor coefficients can be expanded as:

$$\underline{a} = \sum_{i=1}^{M} \frac{(\underline{e}_i^*, \underline{h})}{\lambda_i} \underline{e}_i \tag{9}$$

where $\{\lambda_i\}$ and $\{\underline{e}_i\}$ represent, respectively, the eigenvalue and eigenvector set of the covariance matrix. One can now divide the eigenspace into noise and signal subspaces and express the minimum norm solution as a linear combination of the signal space eigenvectors. This, in effect, results in the filtering out of the noise from the estimate.

The Capon estimate (maximum likelihood) is based on designing a filter that minimizes the variance of the output under the constraint that the frequency response at each f_i be equal to a constant value. Finally both the Pisarenko estimate and the Prony line spectrum estimates take into consideration, a priori, that the data consists of sinusoids in noise. In the Pisarenko method, the roots of the polynomials made up of the eigenvector of the autocorrelation matrix corresponding to the smallest eigenvalue are used to estimate the tone frequencies.

4. COMPARISON OF ESTIMATION TECHNIQUES

An existence simulation study has been carried out to determine the probability of error behaviour of the DTMF detector under various noise and signalling conditions. In the simulation runs the tone pairs are randomly selected with relative phases uniformly distributed in $[-\pi, \pi]$ and a random twist factor in the range of +4 to -8 dB. The tone signals are imbedded in Gaussian noise and may further be contaminated by a low density impulsive noise, (i.e., one shot per tone interval), the impulse epochs being also uniformly distributed within the tone interval.

Plots of spectral estimates and probability of error P_e behaviour are shown in Figs. 3 to 10. In these plots N denotes the number of samples used, p, the order of the predictor and the contaminating noise is Gaussian unless otherwise specified. Finally the signal samples are obtained at a sampling rate of 8 kHz, and the tone frequencies are selected as in Table. I.

Autocorrelation method

Plots of spectral estimates and pole configuration using the autocorrelation method are shown in Fig. 3a. The experiments with small predictor orders, e.g., p = 4,6,... indicate a relatively low resolution while the signal poles appear well within the unit circle. As the predictor order is increased, the "signal" poles move onto the unit circle while the "noise" poles are lined up uniformly within the unit circle as they try to model the flat noise spectrum. The probability of error behaviour is shown in Fig. 4 where we see that a model order at or above p = 16 yields very satisfactory results ($N \geq 50$). In fact one has $P_e = 0.5 \times 10^{-5}$ at 7 dB and at 10 dB the projected error is less than 0.5×10^{-7}. Fig. 5 illustrates the effects on P_e of the number of samples used and also that of the predictor order, p. Here one can observe the threshold behaviour of the nonlinear estimator. In Fig. 6 we have illustrated the effects of the frequency separation and the relative phase. It is

of interest to note that P_e behaviour follows the fluctuations of the Cramer-Rao bounds as in Fig. 2, with the relative phase. We have scaled the frequency axis by a factor α, thereby obtaining different tone frequency separations. For $\alpha>1.3$ we observe that the probability of error approaces that of a single tone; however as the tone frequencies get closer to each other, e.g., $\alpha<0.7$, the sinusoids start interacting so strongly that the detector becomes unable to make correct decisions.

Burg and LS Method

Sample spectral plots with LS algorithm are shown in Fig. 3b. The signal poles are located very close to the unit circle, while the noise poles seem to be widely dispersed around the unit circle. Occasionally some noise pole may wander onto the unit circle causing a spurious peak. Despite the higher resolution obtained the probability of error behaviour with both the LS and Burg techniques has been disappointing as illustrated in Fig. 7. Apart from the increased statistical instability resulting in larger twist values and more deviation in the peak positions the poor P_e performance is, ironically, mostly due to the very high resolution of these spectral estimates. Indeed the DFT grid in (6) for, e.g., 1024-point transform is only 8 Hz while the 3 dB bandwidths of the spectral peaks are fractions of a Hz. This problem is somewhat alleviated by windowing the predictor coefficients with an IIR window (e.g. $\sin\pi Bt/\pi t$) [9]. the choice of the smoothing aperture is not very critical and values of B from 12 to 32 Hz seem appropriate.

Kumaresan-Prony Method

The Kumaresan-Prony method reduces the effects of noise significantly as shown in Fig. 3d, where the noise poles are now much more clustered. The peak-background separation appears to be often less than the other autoregressive schemes and the P_e performance does not improve significantly over the LS method, mostly because the problems that affect LS technique are also present with this method.

Prony and Pisarenko Method

Both of these techniques yield line spectra, hence poles located entirely on the unit circle (Fig. 3e). However both techniques appear extremely sensitive to noise and in particular the Pisarenko technique to the finiteness of the data. Indeed with the Pisarenko method, acceptable P_e figures could be obtained only with sample sizes greater than 1000! With the Prony method it was useful to work with a predictor order above the actual signal; in fact at 20 dB SNR, the probability of error decreased by three decades as p was chosen 6 or 8 as compared to p=4 which is the number of complex exponentials. While going beyond p>10 did not pay off, even for p=6,8, the spurious harmonic(s) would show up in the other tone regions, thus complicating the detection problem.

Comparison of Results

The comparative probability of error behaviour of a DTMF receiver using nonlinear spectrum estimation techniques is shown in Fig. 8, while Fig. 3 shows how the P_e improves with increasing number of data samples. The autocorrelation method performs considerably better than all other techniques;in fact it is the only technique that yields acceptable error probability. It is on interest to note in Fig. 9 how slowly the performance improves by increasing the number of samples used with such techniques as Prony and Pisarento.

Impulsive Noise

In the presence of impulsive noise the P_e performance deteriorates dramatically. For example, at $P_e = 10^{-4}$, the receiver incurs a loss of 15 dB SNR in the presence of impulsive (equal amounts of shot and Gaussian noise) noise as compared to pure Gaussian noise. When the incoming signal is processed through a zero-memory nonlinearity (e.g., a clipper)

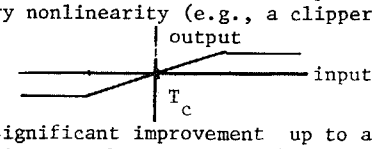

there is significant improvement up to a point where specifications can be met. For the clipper nonlinearity shown above, the performance does not seem to be very sensitive to the threshold setting, through T_c set 3 to 5 dB above the signal level gives the best results.

CONCLUSIONS

DTMF receivers based on nonlinear spectral estimation algorithms have been investigated. Despite their superresolution property these algorithms have not been performing satisfactorily in typical telephone environments. This is mostly due to the fact that the estimation algorithms are inherently very sensitive to noise. We observe that the superresolution property can turn out to be a handicap in an AR based spectrum analyzer as the DFT grid can miss the peaks. We note also that the autocorrelation method of AR parameter estimation is an attractive alternative for DTMF receiver implementation.

REFERENCES

1) J.R. Boddie, N. Sachs, N. Tow, "Receiver for Touch-Tone Service", Bell Sys. Tech. J., 60, 1573-1583, (1981).
2) J.N. Denenberg, "Spectral Moment Estimators: A New Approach to Tone Detection", Bell Sys. Tech. J., 55, 145-155 (1976).
3) J.J. Friend, "Multifrequency Tone Detector",US Patent No. 3,537,001, Oct. 1970.
4) I. Koval, G. Gara, "Digital MF Receiver Using Discrete Fourier Transform", IEEE Trans. Comm., COM-21, 1331-1335, (1973).
5) J.W. Modestino, B. Sankur, "Modelling and Analysis of Impulsive Noise: Part I", Arch. Elek. und Ubertragungtechnik, 35, 481-488, (1982).
6) D.C. Rife, R.R. Boorstyn, "Multiple Tone Parameter Estimation from Discrete-Time Observations", Bell Sys. Tech. J., 55, 1389-1411, (1976).
7) S.M. Kay, S. Marply, "Spectrum Analysis: A Modern Perspective", Proc. IEEE, 69, 1380-1419, (1981).
8) D.T. Tufts, R. Jumaresan, "Estimation of Frequencies of Multiple Sinusoids: Making Linear Prediction Perform Like Maximum Likelihood", Proc. of IEEE 56, 975-990, (1982).
9) T. Thong, A. Kareem, "Spectral Window in a MEM Based Spectrum Analyzer", Proc. Int. Acous. Speech Sig. Proc., 1025-1027, Paris, (1982).

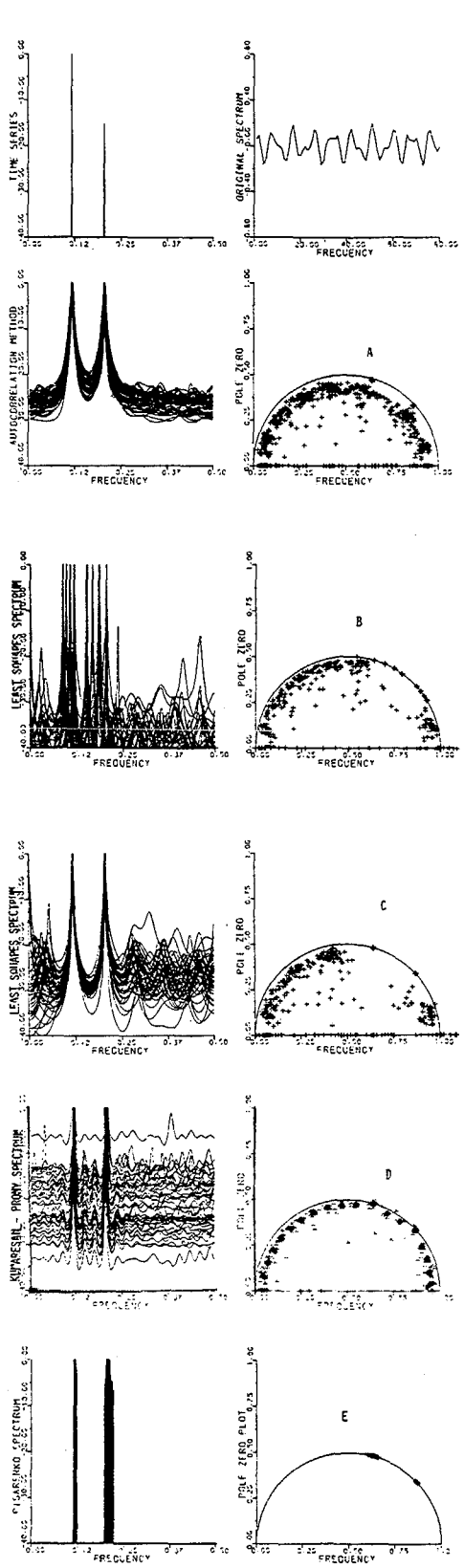

Fig. 3. Sample spectral plots and pole distribution; n = 80, p = 20; SNR = 15 dB. a) The autocorrelation method, b) Least squares method (windowed), d) Kumaresan-Prony method, e) Pisarenko line spectral analysis.

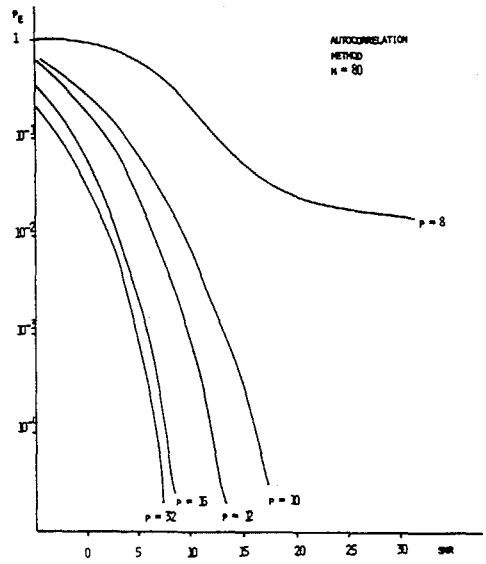

Fig. 4. Probability of error versus SNR: N = 80

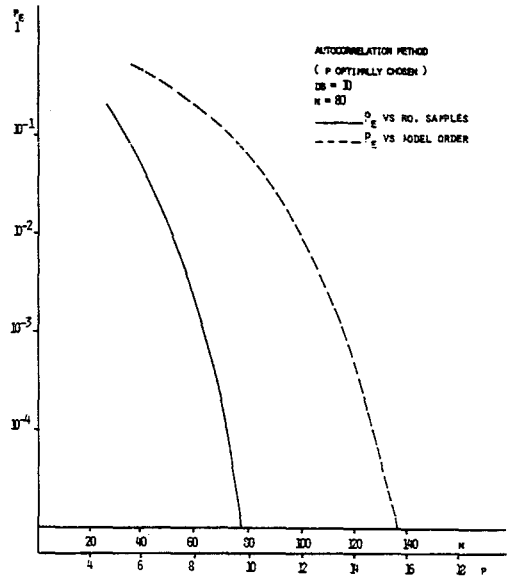

Fig. 5. Probability of error versus the predictor order (solid) and the number of data points (dashed).

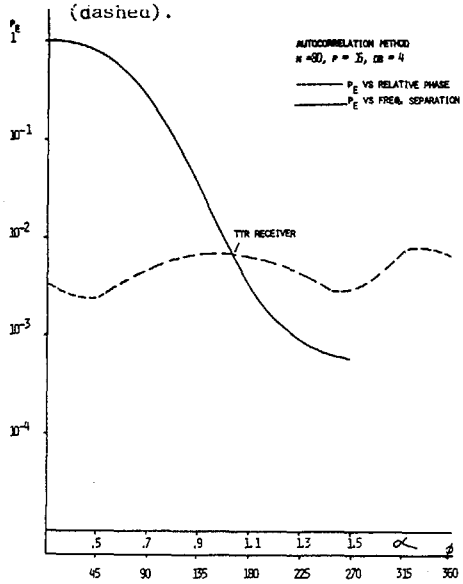

Fig. 6. Probability of error versus relative phase angle and tone frequency separation parameter α

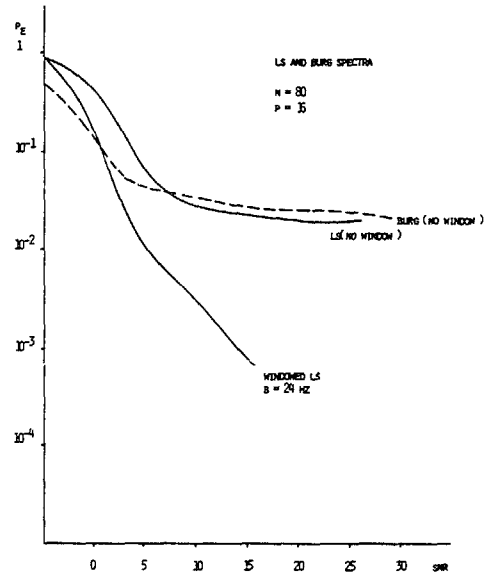

Fig. 7. Probability of error versus SNR using the LS and Burg algorithms.

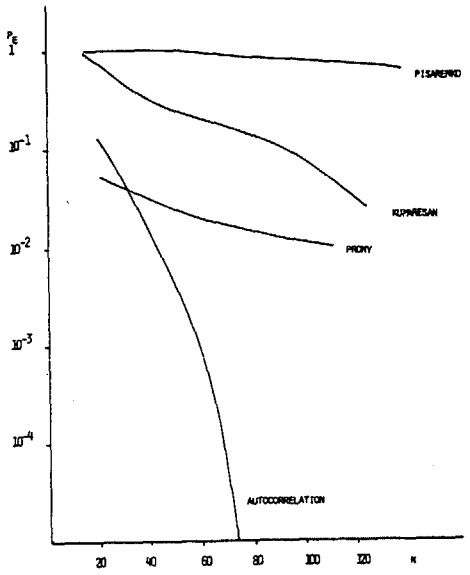

Fig. 9. Probability of error as a function of the number of points used (SNR = 10 dB)

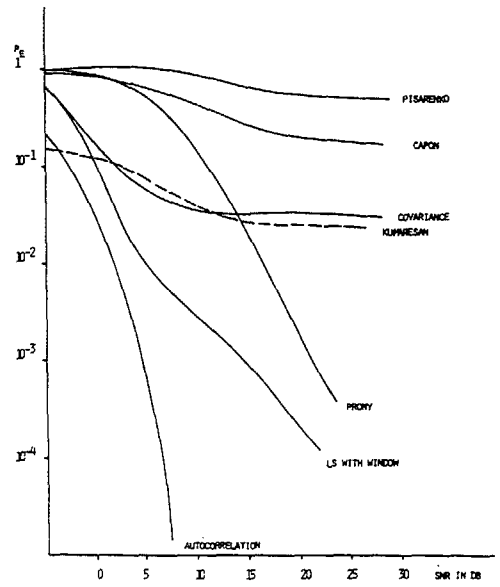

Fig. 8. Comparison of the probability of error using various spectral estimation techniques. N = 80.

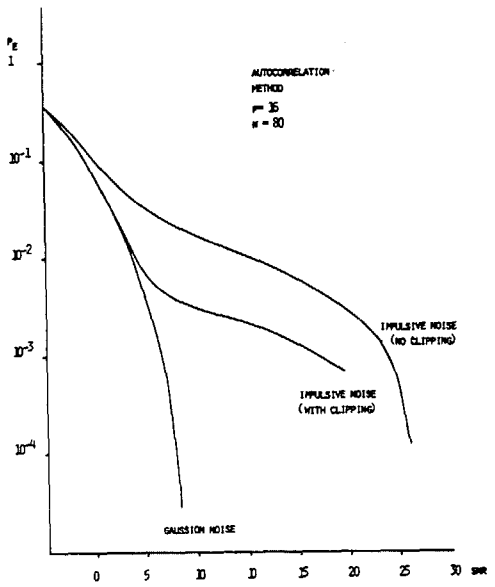

Fig. 10. Probability of error in impulsive noise; p = 16; h(t) = exp(-1200t); power Rayleigh with $\alpha = 0.5$.